DOI: 10.26599/FSHW.2026.9251340

Contents lists available at SciOpen

Food Science and Human Wellness

journal homepage: https://www.sciopen.com/journal/2097-0765

China Food Publishing Co.

Bioorthogonal engineering of an antioxidant-armored probiotic biohybrid potentiates therapy for ulcerative colitis

Xiaomin Chen [1], Huangxin Zhu [2], Zuwei Liu [1], Qianru Zhao [1], Ying Zhang [1*], Hao Wan [1*]

[1] *State Key Laboratory of Food Science and Resources, Nanchang University, Nanchang 330047, China.*

[2] *Department of Gastroenterology, Jiangxi Provincial Key Laboratory of Digestive Diseases, Jiangxi Clinical Research Center for Gastroenterology, Digestive Disease Hospital, The First Affiliated Hospital, Jiangxi Medical College, Nanchang University, Nanchang, Jiangxi, China.*

ABSTRACT: Oral administration of probiotics represents a promising therapeutic strategy for ulcerative colitis (UC), offering the potential to modulate gut immunity and restore mucosal homeostasis. However, the clinical efficacy of conventional probiotics is fundamentally limited by their susceptibility to the pathological oxidative stress within the inflamed intestine, which severely compromises their viability and function. To overcome this critical barrier, we developed a bioorthogonal engineering strategy to construct a robust probiotic-based biohybrid, Lr-DRA. This was achieved by metabolically labeling *Lactobacillus reuteri* (Lr) with azido groups, followed by site-specific, covalent conjugation of a potent phenolic antioxidant, DBCO-modified rosmarinic acid (DRA). This design ensures the stable integration of therapeutic components without impairing probiotic vitality. In a murine model of dextran sulfate sodium (DSS)-induced colitis, orally administered Lr-DRA demonstrated superior therapeutic efficacy. The surface-anchored DRA exerted protective effects by neutralizing oxidative stress. This protective action significantly enhanced the survival and colonization of the probiotic carrier Lr. Consequently, Lr-DRA treatment markedly alleviated clinical symptoms, suppressed pro-inflammatory cytokines, restored intestinal barrier integrity (as evidenced by upregulated tight junction proteins Zonula Occludens-1 [ZO-1] and Occludin), and promoted mucosal healing. This work establishes a versatile and modular platform for fabricating advanced living therapeutics. By simply varying the probiotic chassis and the conjugated bioactive payload, this strategy can be readily adapted to develop targeted treatments for a broad spectrum of gastrointestinal and metabolic disorders.

Keywords: Oral probiotic; Ulcerative colitis; Antioxidant; Bioorthogonal engineering

1. Introduction

Ulcerative colitis (UC) is a chronic illness of the digestive system. Its main feature is constant irritation in the lining of the large intestine[1]. A hallmark of its pathogenesis is the massive overproduction of reactive oxygen species (ROS) within the intestinal microenvironment[2]. This oxidative surge not only directly damages epithelial cells and disrupts the critical intestinal barrier but also perpetuates inflammatory signaling cascades, thereby establishing a vicious cycle that drives disease progression[3]. Conventional pharmacological interventions for UC, such as aminosalicylates, corticosteroids, and biologic agents,

***Corresponding author**
zhangying908@163.com(Y. Zhang).
wanhao424@ncu.edu.cn(H. Wan).

Received 12 February 2026
Received in revised from 30 March 2026
Accepted 11 May 2026

primarily aim at suppressing the immune system[4]. However, these approaches are often accompanied by significant side effects, risk of infection, and the potential for diminished response over time[5]. Moreover, they seldom address the fundamental issue of oxidative stress within the gut lumen[6]. Therefore, developing novel strategies that can simultaneously mitigate oxidative damage and modulate inflammation in a safe and targeted manner is of paramount importance.

Probiotic therapy has garnered substantial interest as a lifestyle-compatible, non-invasive, and cost-effective alternative[7]. Orally administered probiotics, particularly *Lactobacillus* strains, can modulate the gut microbiota, reinforce the epithelial barrier, and exert immunoregulatory effects[8]. However, a major challenge hindering their efficacy in UC is their vulnerability to the very pathological environment they are intended to treat[9]. The excessive ROS in the inflamed intestine can severely compromise probiotic viability and functionality upon arrival, significantly attenuating their therapeutic potential[10]. Therefore, endowing probiotics with enhanced ROS-scavenging capacity represents a crucial therapeutic goal to ensure their survival and amplify their beneficial effects. Traditionally, enhancing specific traits in probiotics, such as antioxidant activity, has relied on genetic engineering[11]. While powerful, this approach is often time-consuming, technically demanding, and faces regulatory hurdles for clinical translation[12]. As an attractive alternative, chemical modification of the bacterial surface offers a more straightforward and controllable route to impart new functionalities[13]. However, conventional chemical conjugation methods often involve harsh conditions or non-specific reactions that can impair the viability, structural integrity, and native probiotic properties of these delicate living cells[13].

Metabolic labeling coupled with bioorthogonal chemistry emerges as an ideal solution to this dilemma. This strategy involves feeding bacteria non-natural metabolic precursors (e.g., azido-modified amino acids), which are seamlessly incorporated into the cell wall during normal bacterial growth[14]. This grafts abiotic chemical handles (e.g., azide groups) onto the bacterial surface under mild, physiological conditions. Subsequently, these handles can engage in highly specific, rapid, and biocompatible “click” reactions with complementary probes or therapeutic cargos (e.g., with dibenzocyclooctyne, DBCO)[15]. This bioorthogonal approach ensures strong, covalent conjugation without interfering with bacterial viability or the host’s physiological processes. To endow probiotics with potent antioxidant activity, we focused on phenolic acids, a class of natural compounds widely recognized for excellent biocompatibility[16] and strong free radical-scavenging capacity[17]. Among them, rosmarinic acid (RA) was selected because of its multifunctional nature. Structurally, RA contains multiple phenolic hydroxyl groups that are associated with strong antioxidant activity, and previous studies have reported higher radical-scavenging capacity than several simpler phenolic compounds, including caffeic acid[18]. Beyond direct ROS scavenging, RA has also been shown to improve intestinal epithelial barrier integrity by upregulating tight junction proteins such as Zonula Occludens-1 (ZO-1) and Occludin, while suppressing NF-κB-related inflammatory signaling[19]. These activities are highly relevant to the pathogenesis of UC. To keep this protection localized and durable, RA was modified with DBCO, yielding DRA. This design allows covalent tethering onto azide-labeled Lr through

copper-free click chemistry. Free RA would readily diffuse in the gut lumen, while surface-anchored DRA remains co-localized with the probiotic carrier, giving rise to a sustained antioxidant shield throughout intestinal transit.

Herein, we report the development of a metabolically engineered probiotic, Lr-DRA, designed to overcome the challenge of pathological oxidative stress in UC. Guided by a design rationale, we first employed metabolic labeling to seamlessly incorporate azido groups onto the surface of the probiotic *Lactobacillus reuteri* (Lr). Subsequently, we harnessed a bioorthogonal copper-free click reaction to covalently conjugate DBCO-modified RA (DRA), a potent natural polyphenol antioxidant, onto the bacterial surface, yielding the final therapeutic agent Lr-DRA. Upon oral administration, the surface-anchored DRA would exert protective effects by neutralizing oxidative stress in the inflamed intestinal microenvironment. This serves a dual purpose: it directly neutralizes oxidative damage to the host tissue and simultaneously creates a protective niche that enhances the survival and functionality of the probiotic Lr carrier. The viable Lr then exerts its inherent beneficial effects, including reinforcing the intestinal epithelial barrier and modulating local immune responses. As a result, in a dextran sulfate sodium (DSS)-induced mouse model of UC, oral treatment with Lr-DRA demonstrated superior therapeutic efficacy. It significantly alleviated disease symptoms (reduced body weight loss and colon shortening), restored colon tissue architecture, and enhanced the expression of tight junction proteins (ZO-1 and Occludin) to rebuild barrier integrity. The treatment also effectively reduced colonic oxidative stress and downregulated pro-inflammatory cytokine levels. Collectively, this study presents a novel and effective strategy for treating UC by bioorthogonally arming a native probiotic with a therapeutic payload. Our work not only validates Lr-DRA as a promising therapeutic candidate but also establishes a versatile and mild chemical platform for endowing living biologics with enhanced, target-specific functionalities to combat complex inflammatory diseases.

2. Materials and methods

2.1 Materials

MRS medium was purchased from Hopebio Co., Ltd. (Qingdao, China). 3-Azido-D-alanine hydrochloride (HADA) was sourced from Aladdin (Shanghai, China). DBCO-NH_2, N-hydroxysuccinimide (NHS), and *N*-(3-dimethylaminopropyl)-*N'*-ethylcarbodiimide hydrochloride (EDC·HCl) were obtained from Sigma-Aldrich (St. Louis, USA). DCFH-DA was acquired from Shanghai Meryer Biochemical Technology Co., Ltd. (Shanghai, China). ELISA kits for MPO and cytokines (IL-6, TNF-α, IL-10) were supplied by Shanghai Keshun Biotechnology Co., Ltd. (Shanghai, China). DSS (molecular weight 36,000–50,000 Da) was provided by Alfa Aesar (Ward Hill, USA). Hydrogen peroxide (H_2O_2, 30%) was from Sinopharm Chemical Reagents (Shanghai, China). All other reagents used were of analytical grade and commercially available.

2.2 Synthesis of DBCO-modified RA (DRA)

DRA was synthesized via a two-step EDC/NHS coupling reaction. First, RA (0.0555 mmol) and NHS (11.5 mg) were dissolved in anhydrous *N*,*N*-dimethylformamide (DMF, 3 mL) in an ice bath (0 °C) under

nitrogen protection. EDC·HCl (0.0999 mmol) was then added in one portion. The mixture was stirred in the ice bath for 30 min before warming to room temperature and stirring for an additional 30 min to complete the activation. Subsequently, DBCO-NH_2 (0.03885 mmol) and *N*,*N*-diisopropylethylamine (DIPEA, 0.3552 mmol) were added to the reaction. The conjugation was allowed to proceed at 30 °C with continuous stirring for 48 h. The crude product was purified by preparative high-performance liquid chromatography (HPLC) using a C18 column. Separation was achieved with a gradient of solvent A (0.1% phosphoric acid in water) and solvent B (methanol) at a flow rate of 0.6 mL/min: 5–60% B over 0–10 min, 60–85% B over 10–60 min, 85–95% B over 60–60.1 min, 95% B held for 60.1–65 min, then returned to 5% B over 65.1–70 min. The fraction corresponding to the retention time of 24–26.578 min was collected as the target compound DRA. After solvent removal under reduced pressure, DRA was obtained as a light brown solid. The identity and purity of the final product were confirmed by liquid chromatography-mass spectrometry (LC-MS), which showed the characteristic peak corresponding to the expected $[M+H]^+$ ion at m/z 619.

2.3 Synthesis and characterization of Lr-DRA

Lr-DRA was synthesized by adding 400 μL of Lr to 10 mL of culture medium supplemented with 6 mM HADA, followed by incubation with shaking at 37 °C. After centrifugation (6000 rpm, 3 min), the collected Lr precipitate was washed twice with phosphate-buffered saline (PBS, pH 7.4). The washed cells were then reacted with DRA (1 mg/mL) for 4 h via click chemistry to obtain Lr-DRA. To confirm successful grafting, the zeta potentials of Lr and Lr-DRA were measured using a Zetasizer (Malvern, UK).

2.4 In vitro ROS detection

RAW264.7 macrophages were seeded in 24-well plates at a density of 2×10^5 cells per well and allowed to grow until they reached approximately 80% confluence. Following stimulation with lipopolysaccharide (LPS, 1 μg/mL), the cells were treated with either PBS or Lr-DRA. For the Lr-DRA treatment, 500 μL of a bacterial suspension at 1×10^8 CFU/mL in PBS was added to each well, and an additional 500 μL of PBS was subsequently added, resulting in a total well volume of 1 mL and a final bacterial concentration of 5×10^7 CFU/mL. To evaluate intracellular ROS levels, cells were stained with the fluorescent probe DCFH-DA. Briefly, the culture medium was removed and replaced with 1 mL/well of DCFH-DA solution (5 ng/mL in fresh medium). Following a 30-min incubation in the dark at 37 °C with gentle agitation every 3–5 min, cells were washed three times with PBS. Fluorescence intensity was visualized and imaged using an Olympus IX83 inverted microscope (Olympus, Japan).

2.5 In vitro oxidative stress resistance

Lr and Lr-DRA were exposed to 1 mM H_2O_2 for 2 h under continuous shaking (180 rpm, 37 °C). At designated time points, 100 μL aliquots were collected, centrifuged (6000 rpm, 4 °C, 5 min), and the pelleted cells were washed. After serial dilution in sterile PBS, the samples were plated on MRS agar for CFU enumeration.

2.6 Assessment of antioxidant capacity

The inherent antioxidant activities of Lr and Lr-DRA were evaluated using three complementary chemical assays.

DPPH Radical Scavenging Assay: The antioxidant activity of bacterial samples was evaluated by measuring their ability to scavenge the stable 1,1-diphenyl-2-picrylhydrazyl (DPPH) radical, following a previously described method with minor modifications[20]. Briefly, each sample was mixed with 3 mL of a 500 μM ethanolic DPPH solution. The mixture was kept in the dark for 30 min, after which the absorbance at 517 nm was recorded using a UV-Vis spectrophotometer. We derived the DPPH scavenging activity by applying the following formula:

$$\text{DPPH scavenging （%）} = \frac{A_B - A_H}{A_B} \times 100\%$$

where A_B is the absorbance of the blank control (DPPH solution only) and A_H is the absorbance of the sample (Lr or Lr-DRA with DPPH).

ABTS and FRAP Assays: The 2,2'-azino-bis(3-ethylbenzothiazoline-6-sulfonic acid) (ABTS) radical cation scavenging activity and the ferric reducing antioxidant power (FRAP) were determined using commercial assay kits (Beyotime Biotechnology) in accordance with the provided protocols. Absorbance was recorded at 734 nm for the ABTS assay and at 593 nm for the FRAP assay.

2.7 Stability of Lr-DRA in simulated gastrointestinal fluids

The functional stability of the DRA coating under physiological digestive conditions was investigated by exposing Lr-DRA to simulated gastric and intestinal fluids in sequence. Simulated gastric fluid (SGF) was prepared by dissolving 2.0 g NaCl and 3.2 g pepsin (from porcine gastric mucosa) in deionized water, followed by pH adjustment to 2.5 with HCl and volume adjustment to 1 L. Simulated intestinal fluid (SIF) was prepared in PBS (pH 7.0) with pancreatin added until the final trypsin activity reached 100 U/mL. Lr-DRA, adjusted to 1×10^8 CFU/mL, underwent incubation in SGF at 37 °C for 2 h with gentle shaking at 100 rpm. The treated bacteria were next pelleted by centrifugation (6000 rpm, 5 min), rinsed once in PBS, and transferred into an equivalent volume of SIF for another 2 h incubation at 37 °C. After completion of the digestion sequence, centrifugation was performed again, followed by two PBS washes, and the bacterial suspension was restored to its initial volume. Residual antioxidant activity of the recovered Lr-DRA was then determined using DPPH, FRAP, and ABTS assays as outlined in Section 2.6. Freshly prepared Lr-DRA served as the reference control and was assigned 100% activity.

2.8 Animals

Male C57BL/6J mice (SPF grade, 6–8 weeks old, 20 ± 0.2 g) were obtained from GemPharmatech Co., Ltd. (Nanjing, China). All animals were maintained under controlled conditions (23 ± 3 °C, 55 ± 10% humidity, 12 h light/12 h dark cycle), and the experimental protocol was approved by the Institutional Animal Care and Use Committee of Nanchang University (approval no. NCULAE-202601010099).

2.9 In vivo toxicity analysis

Male C57BL/6J mice were divided randomly into two groups and administered daily with PBS or Lr-DRA (1×10^{10} CFU/mL) via oral gavage over a 10-day period. Blood and multiple organ samples were subsequently collected at the endpoint for further analysis.

2.10 In vivo fluorescence imaging of probiotic gastrointestinal retention

To determine whether DRA modification improves the gastrointestinal persistence of Lr, fluorescently labeled bacteria were prepared and then monitored *in vivo* after oral administration. Surface azide groups were introduced by culturing Lr with 6 mM HADA to generate Lr-N_3. After that, the azide-labeled bacteria were incubated at room temperature for 4 h under gentle shaking with DBCO-Cy7.5 (20 μM in PBS) to obtain Lr-Cy7.5, or with DBCO-RA to produce dual-labeled Lr-DRA-Cy7.5.

Residual reagents were removed through centrifugation at 6000 rpm for 3 min, followed by three washes with sterile PBS. Healthy female C57BL/6J mice aged 6–8 weeks were fasted for 12 h before imaging in order to reduce background autofluorescence from chow. Each mouse then received a single oral gavage of fluorescently labeled bacteria in a total volume of 200 μL, with the bacterial concentration adjusted to 1×10^9 CFU/mL in PBS. Whole-body fluorescence imaging was performed using an *in vivo* imaging system (DeepVision, Nirmidas Biotech) at 12 h after administration. All images were acquired under identical exposure conditions, with excitation at 780 nm and emission collected using a 1000 nm long-pass filter at 12 h time points across all experimental groups.

2.11 Therapeutic effect of Lr-DRA on DSS-induced UC

Following a 7-day acclimatization period, C57BL/6J mice (n=5 per group) were randomly assigned to six groups: normal, model, DRA, Lr, Lr + DRA, and Lr-DRA. UC was induced by providing 3% DSS in drinking water for 5 days, while the normal group received plain water throughout. After DSS removal, mice were treated daily via oral gavage (200 μL) for 5 days according to their group designation. Mice in the Lr and Lr-DRA groups received bacterial suspensions (1×10^{10} CFU/mL in PBS). The DRA group was given an equivalent amount of DRA as contained in Lr-DRA. In the Lr + DRA group, a freshly prepared mixture containing the Lr suspension and DRA solution at the same respective doses was made immediately before gavage, after which the combined preparation was delivered in a single oral administration with a total volume of 200 μL. The normal and model groups received PBS (200 μL/day). 12 h after the final gavage, all mice were weighed, euthanized, and colon length was recorded. Distal colon segments were fixed in 4% paraformaldehyde for histology. Serum was isolated by centrifugation, and both colonic contents and serum were stored at −80 °C for subsequent analysis.

2.12 Disease activity index (DAI) assessment

Throughout the experimental period, stool consistency, fecal bleeding, and changes in body weight were recorded daily. Each parameter was scored based on established criteria, and the scores were used to calculate the DAI.

2.13 Immunofluorescence staining

Colon sections were deparaffinized and subjected to immunofluorescence staining for ZO-1 and occludin. Following an overnight incubation with primary antibodies at 4°C, the sections were washed thoroughly using PBS (pH 7.4). Subsequently, fluorophore-conjugated secondary antibodies were applied and incubated for 60 min at room temperature. Finally, nuclei were counterstained with DAPI, and images were acquired using fluorescence microscopy.

2.14 Quantification of serum biomarkers via ELISA

After separating the serum by centrifuging whole blood at 4°C, the levels of MPO, IL-6, TNF-α, and IL-10 were measured using commercial ELISA kits as instructed.

2.15 Statistical analysis

Data are expressed as mean ± SD. Differences between two groups were assessed using Student's t-test. Comparisons among three or more groups were performed using one-way ANOVA. For one-way ANOVA that yielded a significant result, post hoc comparisons were conducted using Dunnett's multiple comparisons test to compare all experimental groups against the control group. Statistical significance was set at $*P < 0.05$, $**P < 0.01$, $***P < 0.001$, and $****P < 0.0001$.

3. Results

3.1 Bio-orthogonal preparation of Lr-DRA and its characterization

For a proof-of-concept demonstration, the probiotic strain Lr was selected due to its established anti-inflammatory and microbiota-stabilizing functions[21], coupled with its robust capacity for intestinal adhesion and colonization[22]. To fabricate Lr-DRA, azide moieties were initially displayed on the bacterial surface (yielding Lr-N_3) via metabolic incorporation of 3-azido-D-alanine HCl (HADA), utilizing the native biosynthesis machinery. A protective DRA coating was then covalently assembled on Lr through a copper-free click reaction between the surface-exposed azide groups and DBCO-functionalized RA, resulting in the final construct Lr-DRA. This entire preparation strategy is both bioorthogonal and efficient.

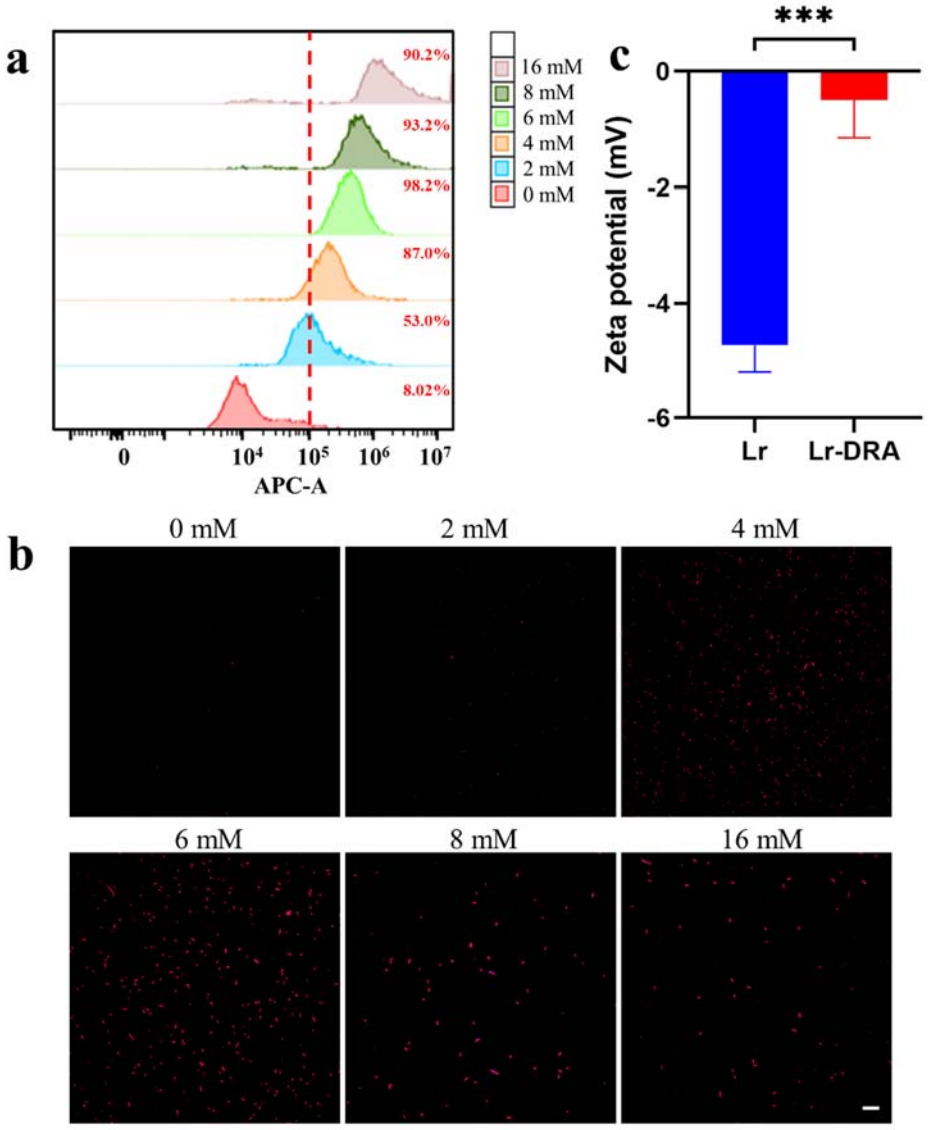


Fig. 1. Characterization of Lr-DRA. (a) Flow cytometric analysis of metabolic labeling of Lr with different concentrations of HADA. (b) CLSM analysis of metabolic labelling of Lr with different concentrations of HADA. Scale bar, 20 μm. (c) Zeta potential characterization of Lr and Lr-DRA (n = 3). Values are presented as mean ± SD. Statistical analyses employed Student's t-test, with significance threshold set at ***$P < 0.001$.

To establish a covalent linkage at the single-cell level for equipping Lr with a phenolic acid-based functional module (DBCO-modified RA, DRA), the optimal concentration of the metabolic precursor HADA was systematically evaluated. The detailed characterization of DRA is provided in Fig. S1. The mass spectrometry analysis (Fig. S1) of DRA reveals the successful conjugation of DBCO to RA. Notably, the major peak at 619.2115 Da corresponds to the expected mass for the DBCO-modified RA, indicating the successful attachment of DBCO. Analytical HPLC of the purified fraction showed a predominant peak, indicating effective enrichment of DRA after purification (Fig. S2). To verify the effective assimilation of HADA by Lr and to determine its optimal concentration, Lr samples incubated with varying amounts of HADA were labeled with a fixed concentration of DBCO-modified AZDye™ 647 fluorophore (DBCO-AF647). As illustrated in Fig. 1a, the labeling efficiency reached near saturation at an HADA concentration of 6 mM, achieving approximately 98.2%. This quantitative outcome was further supported by confocal laser scanning microscopy (CLSM), where strong AF647 fluorescence was observed on the labeled

Lr (Fig. 1b). These findings confirm the successful incorporation of HADA, providing a basis for further functionalization. Following the confirmation of successful metabolic azide labeling on Lr, DRA was covalently conjugated to the bacterial surface via copper-free click chemistry. The successful coating was first corroborated by a significant change in surface charge, as shown in Fig. 1c, the zeta potential increased markedly from -4.73 mV for native Lr to -0.49 mV for Lr-DRA, indicating effective surface modification.

3.2 Resistance of Lr-DRA to oxidative stresses

To exert its therapeutic function in UC, the probiotic must withstand the detrimental oxidative stress prevalent in the inflamed gut. Having successfully synthesized Lr-DRA, we systematically evaluated its ability to resist such adverse conditions. We first assessed the compared antioxidant capacity of Lr and Lr-DRA using standard chemical assays. The results from DPPH (Fig. 2a), FRAP (Fig. 2b), and ABTS (Fig. 2c) scavenging assays consistently demonstrated that Lr-DRA possessed significantly enhanced antioxidant activity compared to unmodified Lr, indicating that the surface-conjugated DRA provides direct radical-quenching capability.

These cell-free assays provide confirmation of the DRA coating's inherent antioxidant capacity in chemical systems, yet they fail to replicate the complex biological environment found in inflamed tissue. We therefore further assessed whether this antioxidant activity could be retained in a cellular context more relevant to inflammatory oxidative stress associated with UC. LPS-stimulated RAW264.7 macrophages, a commonly used *in vitro* model of inflammatory oxidative stress, were stained with the ROS-sensitive probe DCFH-DA[23]. After treatment with Lr-DRA, these LPS-stimulated RAW264.7 cells exhibited significantly diminished fluorescence, with levels approaching those observed in untreated cells, suggesting the effective scavenging of intracellular ROS (Fig. 2d and Fig. S3). This result demonstrates that the antioxidant activity of the DRA coating remains functional in a biologically relevant cellular environment. Encouraged by this cellular protection, we directly tested the tolerance of the bacteria themselves to oxidative assault. Lr and Lr-DRA were exposed to 1 mM H_2O_2 to simulate acute oxidative stress. Strikingly, Lr-DRA exhibited a significantly higher survival rate than native Lr (Fig. 2e), providing direct evidence that the DRA coating protects the probiotic carrier from oxidative damage. In summary, these findings clearly demonstrate that the covalent incorporation of DRA substantially enhances the resistance of Lr to oxidative stress. To further probe the translational potential of Lr-DRA, we tested whether its antioxidant coating could remain stable during simulated gastrointestinal transit. Residual radical-scavenging activity of the surface-conjugated DRA was measured after sequential treatment with SGF for 2 h and SIF for 2 h. As illustrated in Table S1, 100.86 ± 0.76%, 101.40 ± 0.37%, and 95.41 ± 2.87% of the initial activity were still retained by Lr-DRA in the DPPH, FRAP, and ABTS assays, respectively. The strong preservation of antioxidant capacity suggests marked stability of the triazole linkage produced by strain-promoted azide-alkyne cycloaddition (SPAAC) click chemistry, even under acidic hydrolysis and enzymatic degradation conditions. The DRA coating stayed functionally intact as well, giving the probiotic a persistent antioxidant shield during passage through the harsh gastrointestinal environment and before arrival at the inflamed intestine.

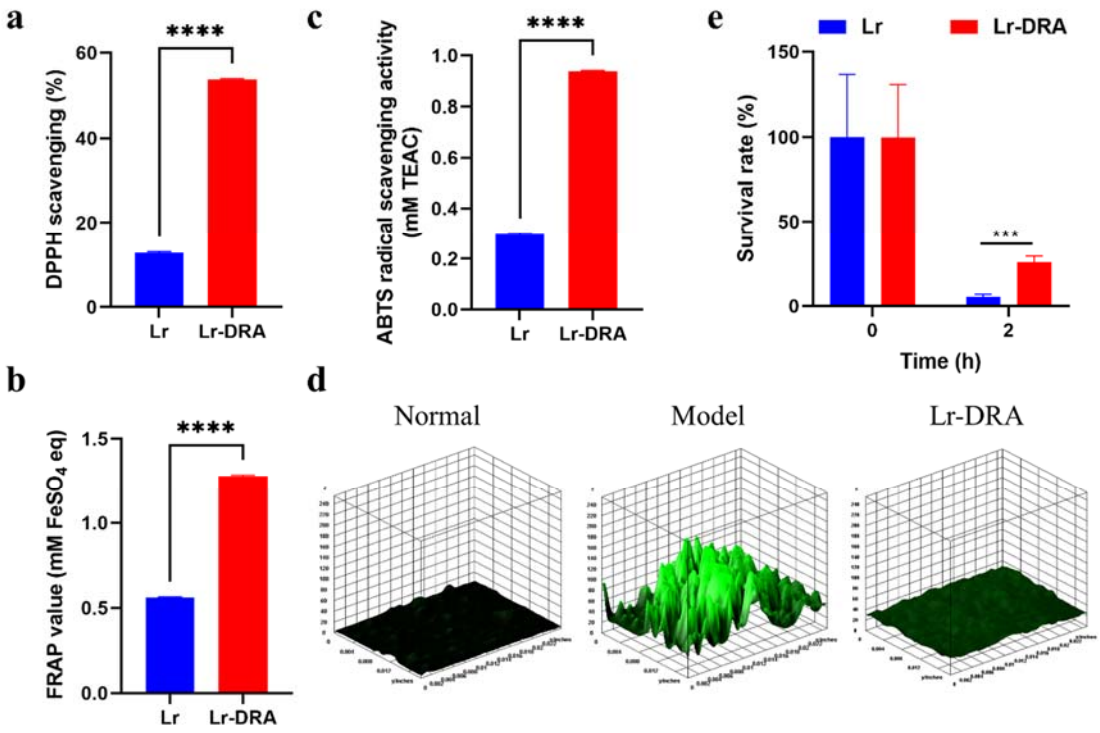


Fig. 2. Evaluation of Lr-DRA resistance against diverse stresses. (a-c) Antioxidant activities of Lr and Lr-DRA evaluated by DPPH (a), FRAP (b), and (c) ABTS assays (n=3). (d) Three-dimensional surface plots visualizing intracellular ROS levels. The plots were generated based on fluorescence intensity from DCFH-DA staining in LPS-stimulated RAW264.7 cells after different treatments. The cells were stained by the ROS probe DCFH-DA (green fluorescence). (e) Relative survival rates of Lr and Lr-DRA after exposure to H_2O_2 (1 mM) (n=3). Data are expressed as mean ± SD. Statistical analyses employed Student's t-test, with significance thresholds set at ***$P < 0.001$ and ****$P < 0.0001$.

3.3 In vivo biocompatible evaluation of Lr-DRA after oral administration

Encouraged by the promising *in vitro* results, we next investigated the *in vivo* performance of Lr-DRA, beginning with an assessment of its systemic biocompatibility (experimental timeline in Fig. 3a). As anticipated, oral administration of Lr-DRA exhibited no detectable toxicity in mice. Key indicators of systemic health remained comparable between treated and control animals throughout the study. Systemic health was comprehensively monitored, including stable body weight profiles (Fig. 3b). Histopathological examination of major organs (heart, liver, spleen, lungs, and kidneys) via hematoxylin and eosin (H&E) staining revealed no signs of tissue damage or inflammation, with architecture indistinguishable from that of untreated controls (Fig. 3c). Finally, analysis of a full panel of serum biochemistry parameters further confirmed its safety profile. These parameters covered markers of liver function (alanine aminotransferase, ALT; aspartate aminotransferase, AST; alkaline phosphatase, ALP; albumin, ALB); kidney function (creatinine, CREA); and cardiac/muscle integrity (creatine kinase, CK; lactate dehydrogenase, LDH), none of which showed significant alterations relative to controls (Fig. 3d-j). Taken together, these findings demonstrate that Lr-DRA possesses an excellent safety profile and remarkable biocompatibility following oral delivery.

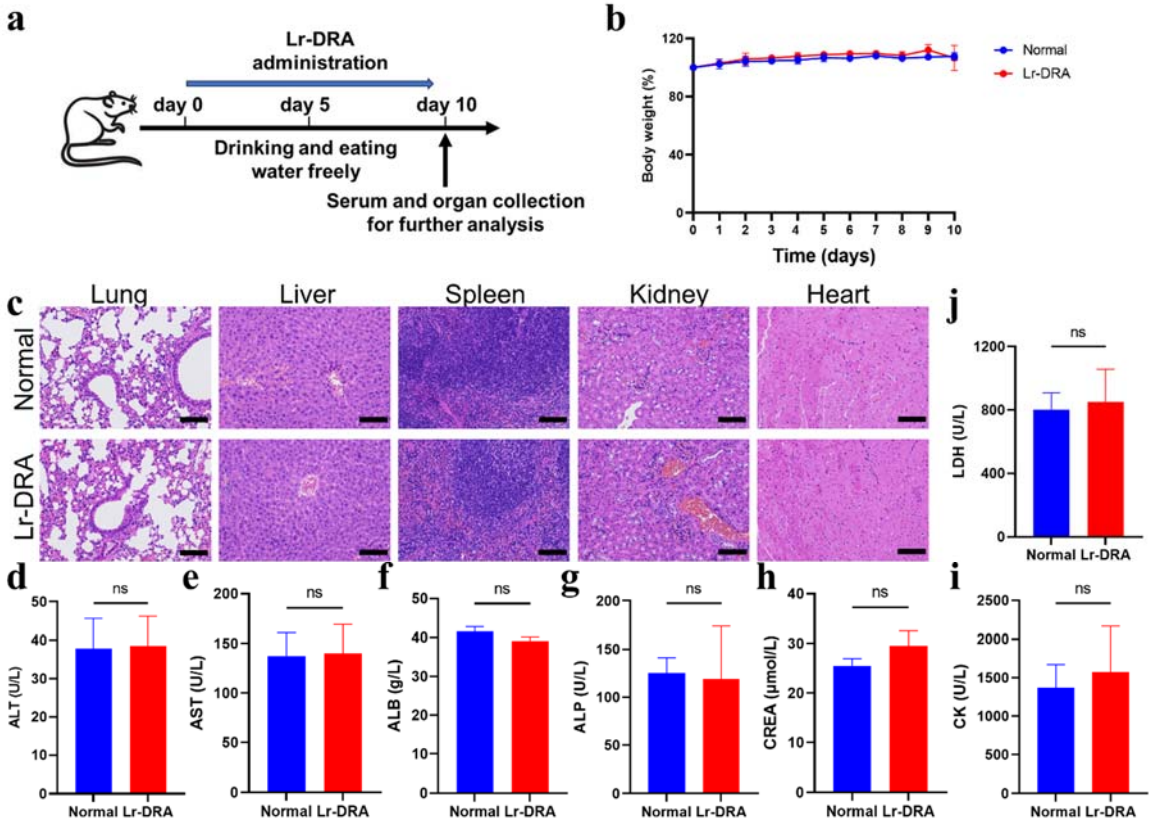


Fig. 3. *In vivo* biocompatible assessment of Lr-DRA. (a) C57BL/6J mice received daily oral gavage of either PBS or Lr-DRA for 10 consecutive days before euthanasia and subsequent biocompatibility analysis. (b) Body weight changes over time in mice with or without Lr-DRA treatment. (c) H&E staining of major organs collected from treated and untreated mice. (d-j) Serum biochemical parameters measured in mice administered with or without Lr-DRA. Data are presented as mean ± SD. Statistical analyses employed Student's t-test. ns: not significant.

Prolonged residence in the gastrointestinal tract is generally considered beneficial for orally administered probiotics to exert sustained therapeutic effect. The influence of DRA modification on the gastrointestinal persistence of Lr was evaluated by longitudinal *in vivo* fluorescence imaging in healthy mice. Surface labeling of Lr was carried out with the near-infrared dye DBCO-Cy7.5 through SPAAC click chemistry, generating the fluorescently traceable preparations Lr-Cy7.5 and Lr-DRA-Cy7.5. After a single oral gavage, whole-body fluorescence signals were monitored for 12 h. As presented in Fig. S4, mice treated with Lr-DRA-Cy7.5 exhibited stronger and more persistent abdominal fluorescence than those receiving Lr-Cy7.5. Quantitative analysis of the abdominal region of interest in Fig. S5 further showed a slower decline of the Lr-DRA-Cy7.5 signal, with the residual signal at 12 h remaining approximately 1.4-fold higher than that in the control groups. These results indicate that covalent conjugation of the DRA antioxidant shield extends the gastrointestinal retention of Lr.

3.4 Therapeutic efficacy of Lr-DRA toward DSS-induced UC in mice

Having fully characterized the functional profile of Lr-DRA, we proceeded to evaluate its therapeutic efficacy against DSS-induced UC in mice. A treatment schedule was established as shown in Fig. 4a. Briefly, mice received 3% DSS in drinking water for 5 consecutive days (days 0–5) to induce UC[24], followed by daily oral administration of PBS, DRA, Lr, a physical mixture of Lr and DRA, or Lr-DRA from day 5 to day 10

(designated as the model, DRA, Lr, Lr + DRA, and Lr-DRA groups, respectively). Normal mice received regular drinking water throughout and were given PBS on days 5–10 (normal group; Fig. 4a). As shown in Fig. 4b and Fig. S6, mice in the normal group exhibited consistent weight gain and minimal disease activity index (DAI) scores throughout the study. In stark contrast, mice in the model group developed severe colitis, characterized by significant body weight loss and a sharp increase in DAI. Body weight loss was significantly ameliorated in the Lr + DRA and Lr-DRA groups. Meanwhile, DAI scores were markedly reduced in three treatment groups (DRA, Lr + DRA, and Lr-DRA), with the most pronounced improvement observed in the Lr-DRA group. We further assessed macroscopic indicators of colitis severity by analyzing colon length (Fig. 4c, d). DSS administration in the model group led to marked colon shortening relative to the normal group. All treatment groups (DRA, Lr, Lr + DRA, and Lr-DRA) showed statistically significant improvements compared to the model group. Among them, Lr-DRA was the most effective. This superior efficacy is likely attributable to the metabolic activity of the DRA-armored Lr, which exhibited superior viability under oxidative stress *in vitro* (Fig. 2e). These results provide preliminary *in vivo* validation for the advantage of bioorthogonal functionalization in enhancing probiotic therapy for UC.

It is noteworthy that oral administration of DRA alone also demonstrated a measurable therapeutic effect against UC. This observation suggests that the intrinsic antioxidant properties of DRA may contribute to disease alleviation and could synergize with the probiotic actions of viable Lr within the Lr-DRA conjugate to achieve enhanced efficacy—a hypothesis consistent with our *in vitro* oxidative stress resistance data (Fig. 2a-e). To further substantiate the superior therapeutic effect of Lr-DRA observed at the clinical and macroscopic levels, we performed histopathological analyses on colonic tissues. Hematoxylin and eosin (H&E) staining combined with Alcian blue/periodic acid–Schiff (AB-PAS) staining provided deeper insights into mucosal restoration (Fig. 4e, f). While treatment with DRA, Lr, or their physical mixture (Lr + DRA) led to partial improvement in colon architecture compared to the model group, the morphology remained suboptimal relative to the normal group. In striking contrast, mice treated with Lr-DRA exhibited near-complete histological recovery. Their colonic sections displayed intact and regularly arranged crypt structures, a high abundance of mucin-producing goblet cells, and minimal inflammatory cell infiltration, collectively indicating a potent capacity of Lr-DRA to promote epithelial repair and restore mucosal homeostasis. Prompted by these findings, we investigated the expression of key tight junction proteins, ZO-1 and Occludin, which are critical for maintaining intestinal epithelial barrier integrity[25]. Qualitative assessment by immunofluorescence staining revealed that, compared to other treatments, Lr-DRA most effectively counteracted the DSS-induced reduction in ZO-1 and Occludin signal in the colon (Fig. 4g, h and Figs. S7, S8). The staining intensity in the Lr-DRA group appeared markedly stronger than in other treatment groups and was comparable to that in the normal group. In summary, these multi-faceted results, encompassing clinical scores, organ metrics, histopathology, and molecular barrier markers, conclusively underscore the robust and comprehensive therapeutic efficacy of Lr-DRA in ameliorating experimental ulcerative colitis.

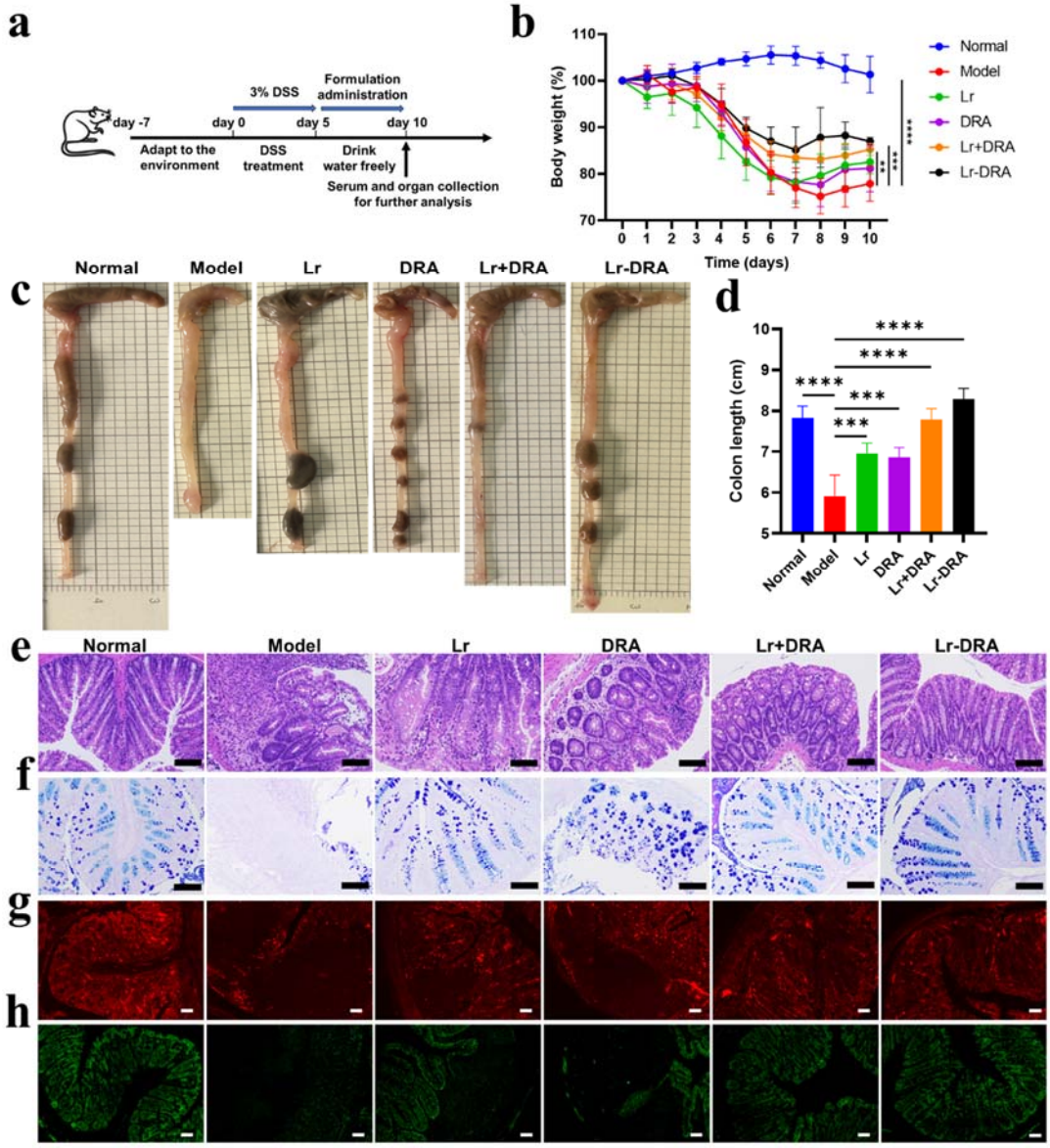


Fig. 4. Therapeutic role of Lr-DRA in DSS-induced murine colitis. (a) Schematic of the experimental timeline for treating DSS-induced ulcerative colitis. After receiving 3% DSS in drinking water for 5 days, C57BL/6J mice were orally administered Lr, DRA, Lr + DRA, or Lr-DRA daily for another 5 days to evaluate treatment efficacy. (b) Body weight changes over time across treatment groups (n = 5). (c, d) Colon images (c) and corresponding colon length measurements (d) collected at the endpoint (n = 5). (e) Representative H&E-stained colon tissue sections obtained on day 10 from each group. Scale bar, 100 μm. (f) AB-PAS staining of colon tissues of mice from different groups. Scale bar, 100 μm. (g, h) Representative immunofluorescence images of the expression of ZO-1 (g) and Occludin (h) in the colon. The red and green channels represented ZO-1 and Occludin, respectively. Scale bar, 50 μm. Data are expressed as mean ± SD. Statistical analyses employed one-way ANOVA with Dunnett's multiple comparisons test. $^{**}P < 0.01$, $^{***}P < 0.001$ and $^{****}P < 0.0001$.

3.5 Therapeutic effects of Lr-DRA on inflammation and oxidative stress

Having validated the therapeutic efficacy of Lr-DRA, we proceeded to investigate its therapeutic effects of Lr-DRA on inflammation and oxidative stress. It is well established that inflammation and oxidative stress form a self-amplifying vicious cycle in UC[26, 27]. Therefore, we measured the concentration of myeloperoxidase (MPO), a neutrophil-derived enzyme that catalyzes the conversion of H_2O_2 into hypochlorous acid (HOCl), a potent ROS. MPO plays a key role in oxidative stress and inflammation,

particularly in neutrophil-mediated immune responses[28]. MPO concentration was markedly elevated in the model group but was significantly reduced by all treatments (DRA, Lr, Lr + DRA, and Lr-DRA) (Fig. 5a). Importantly, the Lr-DRA group exhibited the most pronounced reduction, demonstrating superior efficacy in suppressing this critical amplifier of the inflammation-oxidative stress cycle. The effective neutralization of MPO activity translated into a profound modulation of the inflammatory cytokine milieu. As shown in Fig. 5b-d, Lr-DRA treatment most effectively rebalanced the cytokine profile. It induced the greatest suppression of the pro-inflammatory cytokines tumor necrosis factor-α (TNF-α) and interleukin-6 (IL-6) among all treatment groups, while simultaneously promoting the highest upregulation of the anti-inflammatory cytokine interleukin-10 (IL-10). While the other intervention groups (DRA, Lr, and Lr + DRA) also showed significant modulatory effects compared to the model, their impacts were consistently less pronounced than that of Lr-DRA. This coordinated downregulation of pro-inflammatory signals and enhancement of anti-inflammatory responses underscores the multi-targeted therapeutic action of the bioengineered probiotic.

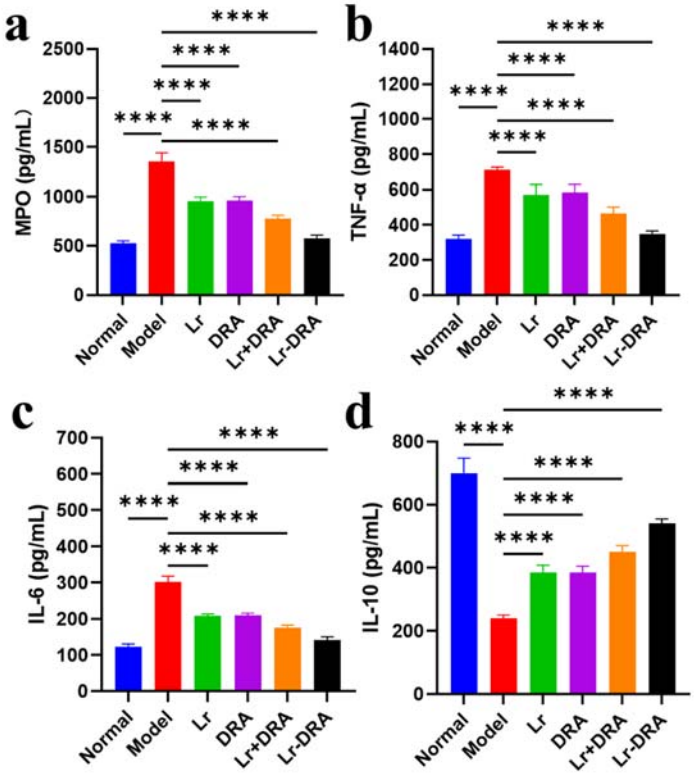


Fig. 5. Anti-inflammatory effects of orally administered Lr-DRA in murine colitis. (a) MPO concentration across experimental groups (n = 5). (b−d) Cytokine concentrations determined by ELISA in each treatment group at endpoint (n = 5). Data are expressed as mean ± SD. Statistical analyses employed one-way ANOVA with Dunnett's multiple comparisons test. ****$P < 0.0001$.

4. Discussion

UC is a chronic and relapsing inflammatory bowel disease characterized by a complex interplay of dysregulated immune responses, impaired epithelial barrier function, and a pathological microenvironment dominated by excessive ROS[29]. This oxidative stress not only inflicts direct damage on intestinal tissues but also perpetuates a vicious cycle of inflammation, presenting a formidable challenge for effective treatment[30]. Current mainstay therapies, including aminosalicylates, corticosteroids, and biologics, often fall short due to

systemic side effects, secondary non-responsiveness, and their limited ability to directly neutralize the luminal oxidative burden[31-33].

In this context, probiotic therapy, particularly employing *Lactobacillus* strains, has emerged as a promising alternative due to its intrinsic ability to modulate gut immunity, reinforce the epithelial barrier, and restore microbial homeostasis in a non-invasive and cost-effective manner. We selected Lr as a model probiotic carrier for its documented therapeutic potential in colitis. However, a critical bottleneck for oral probiotics in UC is their vulnerability to the very hostile, ROS-rich environment they are intended to treat, which can severely compromise their viability and, consequently, their therapeutic efficacy upon reaching the inflamed intestine.

To overcome this limitation, we rationally designed and constructed Lr-DRA, a bioorthogonally engineered probiotic hybrid. This platform leverages metabolic labeling to seamlessly incorporate azido handles onto the Lr surface, followed by highly specific copper-free click chemistry to covalently conjugate DRA. This design imparts several critical advantages: (1) the mild, physiological conditions preserve the native viability and probiotic functions of Lr; (2) the covalent linkage ensures stable and uniform surface decoration of DRA, unlike transient physical adsorption; and (3) DRA, a potent natural polyphenol, is endowed with exceptional antioxidant and anti-inflammatory properties. Upon oral administration, this integrated Lr-DRA system is designed to execute a dual-function strategy. The surface-conjugated DRA shell is endowed with potent ROS-scavenging capacity, which may help mitigate oxidative stress in the gut, while the probiotic Lr core is intended to colonize and exert its beneficial effects. More importantly, the covalent integration of DRA with Lr facilitates a concerted action. By creating a localized antioxidant microenvironment, the DRA shell can shield the adjacent probiotic from oxidative assault—a mechanism directly supported by the enhanced survival of Lr-DRA under H_2O_2 stress. This protected delivery and sustained activity of Lr likely underpin its amplified therapeutic efficacy *in vivo*.

Several approaches have been investigated to improve the oxidative stress resistance of probiotics. Antioxidant enzyme expression can be introduced by genetic engineering, yet translation of this strategy remains limited by regulatory approval issues and low public acceptance of genetically modified organisms. Physical encapsulation offers a certain degree of protection, although the coating often becomes unstable during gastrointestinal transit and the protective effect may not persist long enough. Conventional covalent conjugation has also been used, but bacterial viability is frequently impaired under the harsh reaction conditions required for this type of modification. The metabolic labeling and SPAAC click chemistry platform used in this work differs from those strategies in several important aspects. Mild and bioorthogonal conditions are maintained throughout the reaction process, native probiotic functions remain preserved, and a hydrolytically stable covalent linkage is formed at the same time. RA further strengthens this design, as this naturally derived polyphenol possesses intrinsic anti-inflammatory and barrier-protective properties, making the present system distinct from many biohybrids constructed with synthetic polymers or inorganic nanomaterials. Taken together, the comparison underscores the particular strengths of this strategy, especially

the combination of mild bioconjugation chemistry, preserved probiotic fitness, and disease-relevant therapeutic functionalization.

Our *in vivo* evaluation in a DSS-induced murine UC model unequivocally confirmed the superior therapeutic performance of Lr-DRA. Oral administration of this biohybrid was significantly more effective than free Lr, DRA, or their simple physical mixture (Lr + DRA) in attenuating key clinical manifestations, including body weight loss, DAI elevation, and colon shortening. H&E and AB-PAS analyses further demonstrated that Lr-DRA treatment most effectively restored normal colon architecture and goblet cell abundance. At the molecular level, Lr-DRA potently upregulated the expression of the tight junction proteins ZO-1 and Occludin, indicating a robust reinforcement of the gut epithelial barrier—a fundamental defect in UC pathogenesis.

Mechanistically, the superior efficacy is directly linked to the integrated functions of Lr-DRA. As evidenced, the biohybrid effectively reduced MPO concentration, directly disrupting the oxidative stress axis. Subsequently, this translated into a favorable immunomodulation, characterized by a significant downregulation of pro-inflammatory cytokines (TNF-α, IL-6) and a concomitant upregulation of the anti-inflammatory cytokine IL-10. This coordinated action—protecting the therapeutic agent and reprogramming the inflammatory milieu—embodies the power of our design.

In conclusion, we have developed a novel and effective strategy for UC treatment by bioorthogonally arming a native probiotic with a therapeutic antioxidant. The Lr-DRA biohybrid successfully addresses the critical challenge of probiotic vulnerability in the inflammatory gut. While this study highlights the promise of the platform, future work could explore its long-term safety, precise pharmacokinetics, and potential for loading other therapeutic cargos. In the context of clinical translation, this bioorthogonal strategy provides a mild and modular approach for engineering living therapeutics, although several limitations should be carefully considered. Ensuring scalable manufacturing under good manufacturing practice (GMP) conditions requires strict quality control to maintain both the consistency of DRA conjugation and the long-term viability of probiotic strains. Long-term biosafety, together with the potential immunogenicity of surface-displayed azido and DBCO moieties, requires thorough evaluation in clinically relevant large-animal models. It is also important to recognize that the DSS-induced acute colitis model has inherent limitations, as it does not fully reproduce the relapsing-remitting characteristics of human UC, thereby emphasizing the necessity of future validation in chronic models or human organoid systems. Successfully addressing these challenges will constitute a key step in advancing this promising platform toward clinical application. Nevertheless, our findings establish a versatile and robust chemical platform for engineering next-generation living therapeutics for inflammatory and other complex gastrointestinal diseases.

Conflict of interest

The authors declare no competing interests.

Appendix A. Supplementary material

Supplementary data to this article can be found online.

Reference

[1] M.A. Guggeis, N.A. Andreani, V.A. López-Agudelo, et al., Cross-species engraftment biases and metabolic divergence in gnotobiotic mice humanized with ulcerative colitis microbiota, Gut Microbes. 17 (2025) 2581445. https://doi.org/10.1080/19490976.2025.2581445.

[2] L. Quan, Y. Ouyang, W. Liang, et al., Probiotic-enhanced porous bio-hybrids with inflammatory targeting, ROS Scavenging, and long-term drug release for ulcerative colitis treatment, Adv. Sci. 12 (2025) e04802. https://doi.org/10.1002/advs.202504802.

[3] K. Zhang, Y. Liang, Q. Chen, et al., Orchestrating gut disorders by oral delivery of a living–synthetic hybrid hydrogel, ACS Nano. 19 (2025) 27825-27844. https://doi.org/10.1021/acsnano.5c08982.

[4] Y. Jiang, H. Xu, J. Wu, et al., A hierarchically assembled oral formulation with drug-convertible carriers for targeted ulcerative colitis therapy through a three-pronged strategy, Adv. Compos. Hybrid Mater. 8 (2025) 280. https://doi.org/10.1007/s42114-025-01362-6.

[5] J. Guo, L. Li, Y. Cai, et al., The development of probiotics and prebiotics therapy to ulcerative colitis: a therapy that has gained considerable momentum, Cell Commun. Signal. 22 (2024) 268. https://doi.org/10.1186/s12964-024-01611-z.

[6] Q. Li, M. Zeng, X. Pu, et al., Melittin-loaded multifunctional nanozyme for ulcerative colitis treatment via enzyme-immunotherapy and ferroptosis inhibition, Adv. Funct. Mater. 35 (2025) e03374. https://doi.org/10.1002/adfm.202503374.

[7] H. Ji, X. Yan, L. Zhang, et al., Prebiotics empower probiotics with gastrointestinal stress resistance for colon-targeted release to synergistically alleviate colitis, J. Control. Release. 380 (2025) 297-316. https://doi.org/10.1016/j.jconrel.2025.01.059.

[8] O.P. Vallejos, S.M. Bueno, A.M. Kalergis, Probiotics in inflammatory bowel disease: microbial modulation and therapeutic prospects, Trends Mol. Med. 31(8) (2025) 731-742. https://doi.org/10.1016/j.molmed.2024.12.005.

[9] F. Cao, L. Jin, Y. Gao, et al., Artificial-enzymes-armed Bifidobacterium longum probiotics for alleviating intestinal inflammation and microbiota dysbiosis, Nat. Nanotechnol. 18 (2023) 617-627. https://doi.org/10.1038/s41565-023-01346-x.

[10] Q. Hu, J. Li, T. Wang, et al., Polyphenolic nanoparticle-modified probiotics for microenvironment remodeling and targeted therapy of inflammatory bowel disease, ACS Nano. 18 (2024) 12917-12932. https://doi.org/10.1021/acsnano.4c00830.

[11] Z. Zhang, H. Niu, Q. Qu, et al., Advancements in Lactiplantibacillus plantarum: probiotic characteristics, gene editing technologies and applications, Crit. Rev. Food Sci. Nutr. 65 (2025) 6623-6644. https://doi.org/10.1080/10408398.2024.2448562.

[12] D.B. Kohn, Y.Y. Chen, M.J. Spencer, Successes and challenges in clinical gene therapy, Gene Ther. 30 (2023) 738-746. https://doi.org/10.1038/s41434-023-00390-5.

[13] L. Wang, J. Liu, Dopamine polymerization-mediated surface functionalization toward advanced bacterial therapeutics, Accounts Chem. Res. 57 (2024) 945-956. https://doi.org/10.1021/acs.accounts.3c00798.

[14] M. Fan, X. Zhang, H. Liu, et al., Reversing immune checkpoint inhibitor–associated cardiotoxicity via bioorthogonal metabolic engineering–driven extracellular vesicle redirecting, Adv. Mater. 36 (2024) 2412340. https://doi.org/10.1002/adma.202412340.

[15] I. Lepori, Y. Oz, J. Im, et al., Bioorthogonal “Click” cycloadditions: A toolkit for modulating polymers and nanostructures in living systems, Reactions. 5 (2024) 231-245. https://doi.org/10.3390/reactions5010010.

[16] S. Sigroha, A. Lather, A. Khatkar, Phenolic acid derivatives as preservatives: synthesis, antioxidant, antimicrobial potential and their preservative effectiveness, Int. J. Pharm. Sci. and Res. 12 (2021) 5526-5537. https://doi.org/10.13040/IJPSR.0975-8232.12(10).5526-37.

[17] H. Yuan, F. Wang, Z. Wang, et al., Natural metal polyphenol nanozyme: free radical scavenging and antioxidation for the treatment of acute kidney injury, ACS Mater. Lett. 5 (2023) 2807-2819. https://doi.org/10.1021/acsmaterialslett.3c00906.

[18] A. Khojasteh, M.H. Mirjalili, M.A. Alcalde, et al., Powerful plant antioxidants: A new biosustainable approach to the production of rosmarinic acid, Antioxidants. 9 (2020) 1273. https://doi.org/10.3390/antiox9121273.

[19] L. Tang, J. Deng, P. Shi, et al., Rosmarinic acid improves intestinal barrier integrity through PI3K/AKT/Nrf2-mediated regulation of tight junction protein expression, Int. Immunopharmacol. 164 (2025) 115380. https://doi.org/10.1016/j.intimp.2025.115380.

[20] S. Baliyan, R. Mukherjee, A. Priyadarshini, et al., Determination of antioxidants by DPPH radical scavenging activity and quantitative phytochemical analysis of ficus religiosa, Molecules (Basel, Switzerland). 27 (2022) 1326. https://doi.org/10.3390/molecules27041326.

[21] Y. Wu, X. Zhang, X. Liu, et al., Galactooligosaccharides and Limosilactobacillus reuteri synergistically alleviate gut inflammation and barrier dysfunction by enriching Bacteroides acidifaciens for pentadecanoic acid biosynthesis, Nat. Commun. 15 (2024) 9291. https://doi.org/10.1038/s41467-024-53144-1.

[22] N. Valeur, P. Engel, N. Carbajal, et al., Colonization and immunomodulation by Lactobacillus reuteri ATCC 55730 in the human gastrointestinal tract, Appl. Environ. Microbiol. 70 (2004) 1176-1181. https://doi.org/10.1128/AEM.70.2.1176-1181.2004.

[23] H. Wang, J.A. Joseph, Quantifying cellular oxidative stress by dichlorofluorescein assay using microplate reader1, Free Radic. Biol. Med. 27 (1999) 612-616. https://doi.org/10.1016/S0891-5849(99)00107-0.

[24] B. Chassaing, J.D. Aitken, M. Malleshappa, et al., Dextran sulfate sodium (DSS)-induced colitis in mice, Curr. Protoc. in Immunology. 104 (2014) 15-25. https://doi.org/10.1002/0471142735.im1525s104.

[25] C. Chelakkot, J. Ghim, S.H. Ryu, Mechanisms regulating intestinal barrier integrity and its pathological implications, Exp. Mol. Med. 50 (2018) 1-9. https://doi.org/10.1038/s12276-018-0126-x.

[26] D.L. Clemens, M.J. Duryee, J.H. Hall, et al., Relevance of the antioxidant properties of methotrexate and doxycycline to their treatment of cardiovascular disease, Pharmacol. Ther. 205 (2020) 107413. https://doi.org/10.1016/j.pharmthera.2019.107413.

[27] X. Qi, Y. Li, Y. Xiang, et al., Hyperthermia-enhanced immunoregulation hydrogel for oxygenation and ROS neutralization in diabetic foot ulcers, Cell Biomaterials. 1 (2025) 100020. https://doi.org/10.1016/j.celbio.2025.100020.

[28] D.K. Min, Y.E. Kim, M.K. Kim, et al., Orally administrated inflamed colon-targeted nanotherapeutics for inflammatory bowel disease treatment by oxidative stress level modulation in colitis, ACS Nano. 17 (2023) 24404-24416. https://doi.org/10.1021/acsnano.3c11089.

[29] T. Kobayashi, B. Siegmund, C. Le Berre, et al., Ulcerative colitis, Nat. Rev. Dis. Primers. 6 (2020) 74. https://doi.org/10.1038/s41572-020-0205-x.

[30] P. Muro, L. Zhang, S. Li, et al., The emerging role of oxidative stress in inflammatory bowel disease, Front. Endocrinol. 15 (2024) 1390351. https://doi.org/10.3389/fendo.2024.1390351.

[31] A.R. Bourgonje, M. Feelisch, K.N. Faber, et al., Oxidative stress and redox-modulating therapeutics in inflammatory bowel disease, Trends Mol. Med. 26 (2020) 1034-1046. https://doi.org/10.1016/j.molmed.2020.06.006.

[32] S. Singh, E.V. Loftus Jr, B.N. Limketkai, et al., AGA living clinical practice guideline on pharmacological management of moderate-to-severe ulcerative colitis, Gastroenterology. 167 (2024) 1307-1343. https://doi.org/10.1053/j.gastro.2024.10.001.

[33] T. Velikova, M. Sekulovski, M. Peshevska-Sekulovska, Immunogenicity and loss of effectiveness of biologic therapy for inflammatory bowel disease patients due to anti-drug antibody development, Antibodies. 13 (2024) 16. https://doi.org/10.3390/antib13010016.